Chemical Physics 83 (1984) 19–31
North-Holland, Amsterdam

PRODUCTION OF STABLE AND AUTOIONIZING O_2^- AND NO^- IONS IN Cs–O_2 AND Cs–NO COLLISIONS

U.C. KLOMP and J. LOS

FOM-Institute for Atomic and Molecular Physics, Kruislaan 407, 1098 SJ Amsterdam, The Netherlands

Received 8 July 1982; in final form 24 August 1983

We present absolute total cross sections for electron and ion production in Cs–NO and Cs–O_2 collisions. The laboratory energy of the cesium atoms varied between 30 and 3000 eV. The branching ratio between electron and ion production in these systems provides a direct measure for the amount of molecular anions which are produced in stable or autoionizing vibrational states. The absolute magnitude of the observed cross sections shows that the ionization process is due to a curve crossing between the potentials of the covalent and ionic ground states. The experiment shows that Cs–NO collisions predominantly lead to production of NO^- ions in the vibrational ground state. For both Cs–NO and Cs–O_2 collisions the distribution over vibrational states of the molecular anions is a function of the collision energy. The experimental results are discussed on the basis of several models.

1. Introduction

Collisions between an atom and a molecule which result in vibrational excitation of the molecule are subject to a considerable amount of scientific research. The main reason for this is that such collisions play an important role in many different physical processes like gas discharges, quenching processes and laser physics.

Two mechanisms can be responsible for the vibrational excitation of a molecule when it collides with an atom. The first one is direct momentum transfer. In this case the force between the molecular nuclei is affected by the vicinity of the atom during the collision, but the system remains in the same electronic state. These collisions can be described by calculating the motion of the molecular nuclei along only one potential-energy surface. The other important mechanism occurs when there is a change of the electronic state of the system during the collision. Then the force between the molecular nuclei changes suddenly because there is a change in the potential-energy surface along which they move. Because in general this will result in a simultaneous change of the vibrational as well as the electronic state of the molecule, this is called a “vibronic” transition.

Vibronic transitions also occur in photon absorption processes. The vibrational state of a molecule generally changes when the absorption of a photon results in an electronic transition. Although there exists some analogy between vibronic transitions in photon absorption processes and those occurring in atom–molecule collisions, one may not push this analogy too far because of two reasons. The first one is that the law of conservation of the total energy imposes different boundary conditions on the vibronic transitions in both cases. A second difference between vibronic transitions due to photon absorption and those occurring in atom–molecule collisions is that the transition time is very short compared to a vibrational period of the molecule for poton absorption, while this time depends on the condition energy in atom–molecule collisions. In atom–molecule collisions the transition time can be a considerable fraction of a molecular vibrational period. In other words: photon absorption always gives rise to vertical transitions, while the transition may be non-vertical in atom–molecule collisions.

The aim of this paper is to present some measurements which clearly illustrate the non-vertical character of vibronic transitions in Cs–NO and Cs–O_2 collisions. Measurements of total and differential cross sections for ion-pair formation in Cs–O_2 collisions provide information about the motion of the molecular nuclei after an electronic transition took place [1,2]. In addition, we measured the branching ratios between electron and ion production in collisions between cesium atoms and O_2 or NO molecules. These measurements are a direct probe for the final distribution over vibrational states of the produced NO^- and O_2^- anions.

Hubers et al. [3] did analogous measurements by determining the branching ratios between X_2^- and X^- production in collisions between alkali atoms and halogen molecules (X_2). They showed that, to a good approximation, the transitions could be considered to be vertical in this case. From our measurements we will deduce that this is certainly not true for Cs–NO and Cs–O_2 collisions.

2. Experimental

The experiments have been performed with a molecular beam machine which was especially designed for measuring absolute total cross sections for electron and ion production in atom–molecule collision [4]. In principle, the vacuum part of this machine consists of four differentially pumped vacuum chambers. For a schematic overview of the apparatus see fig. 1.

2.1. Preparation of the primary beam

The cesium beam, which will be called the primary beam throughout this paper, is generated by a conventional charge-exchange source which has been described previously [5]. It is placed in the first vacuum chamber. Besides the primary beam, which consists of fast neutral cesium atoms, the source also generates a beam of Cs^+ ions and thermal atoms. The ions were removed by means of deflection plates, while a rotating disk velocity selector purged the primary beam from thermal atoms. In front of the source and the collision chamber slits were mounted in order to collimate the primary beam. The laboratory energy of the beam varied between 30 and 3000 eV during the experiments. Between these energies the beam intensity increased from 0.01 nA to 1 nA.

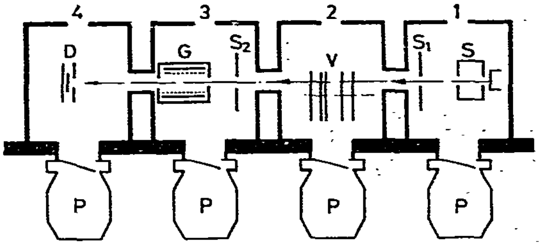

Fig. 1. A schematic diagram of the apparatus. It consists of four differentially pumped vacuum compartments. The first one contains the primary-beam source (S). This beam passes a rotating disk velocity filter (V), and is collimated by two rectangular apertures (S_1) and (S_2), before it enters the collision chamber (G). The primary-beam strength is measured by means of a hot surface ionization detector (D).

2.2. Calibration of the primary-beam energy

The rotating disk velocity selector was also used for calibrating the beam energy. The selector was aligned in such a way that effectively the beam passed through grooves carved in a rigidly rotating drum. The rotation axis was directed along the primary-beam direction. For this configurations the transmission of the primary beam decreases linearly with increasing rotation frequency. When we define F_c as the rotation frequency at which the transmission vanishes, then the beam energy can be calculated according to the formula:

$$E = F_c^2 MA,$$

where E denotes the beam energy and M stands for the mass of the atom. A is a constant which is fixed by the dimensions of the velocity selector. A small misalignment of the selector with respect to the beam direction can be corrected by measuring F_c for opposite rotation directions of the velocity selector.

The beam energy proved to be 10.5–11.5% less than could be expected from the acceleration voltage put on the source. This relative energy deficit was constant throughout the whole energy region in which we did the measurements. This effect has been discussed by Aten and Los [5].

2.3. Detection of the primary beam

A surface ionization detector was used for measuring the primary-beam intensity. This detector consists of a hot rhenium ribbon surrounded by a cylindrical collector. When the primary beam impinges on the rhenium ribbon the atoms are ionized due to surface ionization. To ensure that all ionized cesium atoms reach the collector we maintained a potential difference between the ribbon and the collector. Moreover, in order to collect ions which are reflected from the ribbon with a high kinetic energy, the angle of incidence of the primary beam on the ribbon was chosen to be 45° so that these ions were directly scattered towards the collector. The ion current on the collector was measured with a Keithly electrometer. The working temperature of the ribbon was 1700 K.

The efficiency of the detector must be known in order to measure the cross sections in absolute units. The detection efficiency was measured in an indirect way. The primary beam passed through the collision chamber which was alternately evacuated or filled with Br_2 vapour. It is well known that elastic collisions between cesium atoms and bromine molecules predominantly lead to forward scattering of the Cs atoms [3,6]. Therefore we assume that the attenuation of the primary beam, when it passes through the bromine vapour, is equal to the ion current in the collision chamber. From this equality we can obtain the detection efficiency by dividing the beam attenuation through the ion current. In fig. 2 we show a plot of the detection efficiency as a function of the primary-beam energy. This detection efficiency proved to be unity up to 1000 eV. The decrease at high energies which can be observed in fig. 2 was only reproducible within 10%. It depended on the age of the ribbon and the nature of the gases to which the detector was exposed in previous experiments.

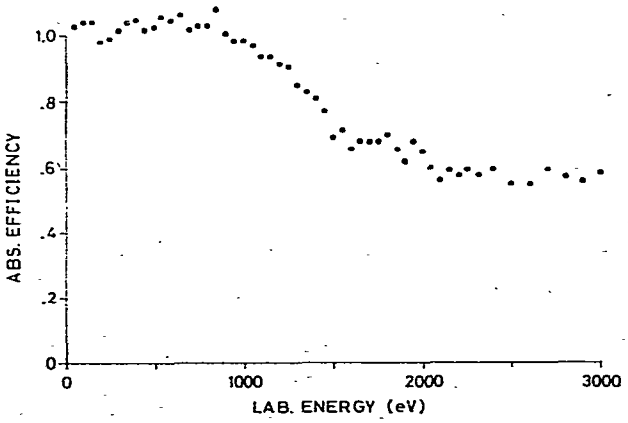

Fig. 2. A plot of the detection efficiency versus the primary-beam energy.

2.4. The collision chamber

In our experiments we used a collision chamber which was previously used by Baede and Los [4], in a modified way. It was differentially pumped in order to obtain background pressures of less than 8×10^{-7} Torr. Typical inlet pressures of the target gas were around 8×10^{-5} Torr during the experiments. It can be seen in fig. 3 that the collision chamber merely consists of two parallel plates between which a set of grids has been mounted. One of the plates is divided into three parts and the middle electrode C acts as the collector plate. This division ensures that the effective collision length is independent of the beam energy and the scattering angle. A potential difference of 300 V, applied between the collector and grid B, deflects

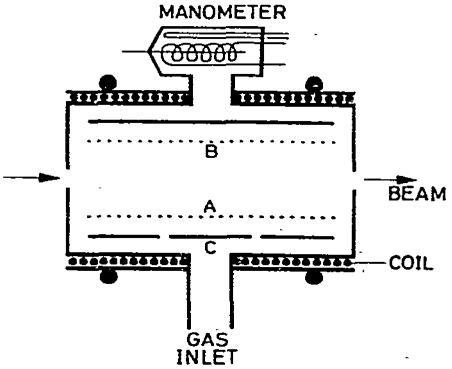

Fig. 3. A schematic diagram of the collision chamber. Electrons and negative ions are measured at the collector (C), by applying a voltage between the two opposite electrodes. The grids (A) and (B) are biased in such a way that secondary electrons produced at these electrodes cannot leave the electrodes. The electrons produced in the interaction region by the collision process can be prevented from reaching the collector by applying a magnetic field pointing along the beam axis.

the electrons and negative ions which are produced in the collision process towards the collector. Grid A is biased at a potential of −30 V with respect to the collector in order to prevent secondary electrons from leaving the collector. These secondary electrons may be produced when the extracted ions and electrons impinge on the collector. A coil surrounds the collision chamber so that a homogeneous magnetic field can be applied in the collision region. The magnetic-field direction points along the primary-beam direction. When this magnetic field is switched on, electrons which are produced in the collision process cannot reach the collector. Because of the large mass of the ions, the magnetic field does not influence the collector current due to ion production. In case of the magnetic field to be switched off, both electrons and ions reach the collector. In order to test if this way of discrimination between electron and ion production worked in the proper way, the primary beam was led respectively through inert gases and bromine vapour. Collisions between cesium atoms and inert-gas atoms can only produce electrons. In this case the total current disappeared when the magnetic field was switched on. This indicates that no electrons were measured as ions. On the other hand, to ensure that no ions were measured as electrons, we let the cesium beam pass through bromine vapour. The magnetic field had no influence on the collector current in this case. This is in agreement with the expectation that cesium–bromine collisions do not lead to electron production.

Considerable care was taken that all the measured currents were in saturation with the voltages applied. It has been confirmed that the collector currents were proportional to the primary-beam intensity and the target-gas pressure.

2.5. *Pressure measurement*

During an experimental run the pressure has been monitored with a calibrated ionization manometer. The calibration has been performed by comparing the readings on the ionization gauge with a Baratron manometer, which was directly connected with the collision chamber. The calibration was done in the 10^{-4} Torr region in which the ionization manometer proved to be linear in target-gas pressure. This made an extrapolation into the 10^{-5} Torr region, in which we did the measurements, readily possible.

2.6. *Experimental procedure*

The experimental procedure in order to obtain the cross sections was as follows:

(1) The primary-beam intensity $I(E)$ was measured as a function of the beam energy E. During this measurement the collision chamber was empty.

(2) Hereafter the target gas was introduced into the collision chamber. We measured the currents on the collector which are caused by the ionization process during the collision as a function of the beam energy. When the magnetic field was switched on we measured the current due to ion production $G_i(E)$. Without the magnetic field the sum of the currents caused by ion and electron production was measured: $G_{i+e}(E)$. Care has been taken that the target-gas pressure was constant during these measurements.

(3) Measurement 1 was repeated in order to control that the beam intensity did not change during the time in which the collector currents were measured.

(4) The ionization manometer was calibrated with the aid of the Baratron in order to obtain the absolute target-gas density N.

Using the following formulas we could calculate the cross sections for ion production $Q_i(E)$ and electron production $Q_e(E)$ as a function of the collision energy:

$$Q_i(E) = \frac{G_i(E) f(E)}{I(E) N L},$$

$$Q_e(E) = \frac{f(E)[G_{i+e}(E) - G_i(E)]}{I(E) N L},$$

where $f(E)$ denotes the detection efficiency and L is the length of the collision region which is equal to the length of the collector. We took the values of the detection efficiency to be equal to those plotted in fig. 2. The formulas for the cross sections Q_i are valid only if the beam attenuation is very small. This attenuation was on the order of a few percent in all cases.

2.7. Limitation of the electron cross-section measurements

Two independent processes may lead to production of electrons in collisions between cesium atoms and NO or O_2 molecules. The first is electron detachment from vibrationally excited anions which are formed by a curve-crossing process. The second process that may lead to electron production is direct ionization. It is known that this process becomes important at high collision energies. In our experiment we cannot distinguish between the two processes.

In order to obtain an impression of the magnitude of the direct-ionization contribution to the electron cross section, we measured the electron production in collisions between cesium and inert-gas atoms. That these collisions lead to electron production via a curve crossing seems improbable. We observed that the thresholds for electron production in these collisions depended on the mass of the inert-gas atom. The lowest threshold had been measured for the Ca–Xe system. It occurred at a laboratory energy of ≈ 300 eV. From the experiments on collisions between cesium atoms and the other inert-gas atoms it could be confirmed that the threshold for electron production was higher in energy if the mass of the inert-gas atom was smaller. The absolute magnitude of the cross sections for electron production did rise to a few Å at a collision energy of 3000 eV. In order to be sure that only electron production due to autoionization of vibrationally excited molecular anions is measured, we report no electron production data for collision energies higher than 300 eV.

2.8. Error estimates

The error in the absolute magnitude of the cross sections is a cumulation of errors made in the pressure, current and detection-efficiency measurements. The pressure measurement is reliable within a few percent which is the maximal deviation of a calibrated Baratron membrane manometer. The currents measured on the collector of the collision chamber and the detector were at least a few times 10^{-12} A. Currents with this magnitude can be measured with considerable accuracy. This means that the main error in the magnitude of the cross section is due to the uncertainty in the detection efficiency. As has been stated before, the magnitude of the detection efficiency is reliable within 10% for energies higher than 1000 eV. From fig. 2 it can be seen that the standard deviation of the detection efficiency is ≈ 5% for energies lower than 1000 eV. Instead of using the calibration points in fig. 2 directly, we constructed a calibration table by drawing a smooth line through these points. It should be noticed that (due to the small beam attenuation) the scattering in the points of the measured detection efficiency is much larger than the scattering of the measured (uncalibrated) cross sections for ion and electron production. For this reason we claim an accuracy of the absolute magnitudes of the cross sections of 10% for energies lower than 1000 eV, and of 15% for higher collision energies.

3. Results

The absolute total cross sections for ion and electron production in collisions between cesium atoms and NO or O_2 molecules are shown in figs. 4A (Cs–NO) and 4B (Cs–O_2) as a function of the (center-of-mass) collision energy. The relative total cross section for ion production in Cs–O_2 collisions has been measured before by Kleyn et al. [2]. Although they applied a different technique, there is good agreement between their and our measurements. The position of the maxima and minima in this cross section are the same for both experiments. Also the overall shape of the cross section as a function of the collision energy coincides in both experiments. We measured, however, a smaller absolute magnitude of the cross section than has been calculated by Kleyn. With respect to this quantity our experiments are reliable because we took considerable care in determining the detection efficiency, absolute target-gas pressure and the length of the scattering region in a direct way.

It can be seen in fig. 4 that there is a difference between the ion-pair formation cross section for collisions between cesium atoms and O_2 molecules and that for Cs–NO collisions. The cross section for ion production in Cs–O_2 collisions exhibits

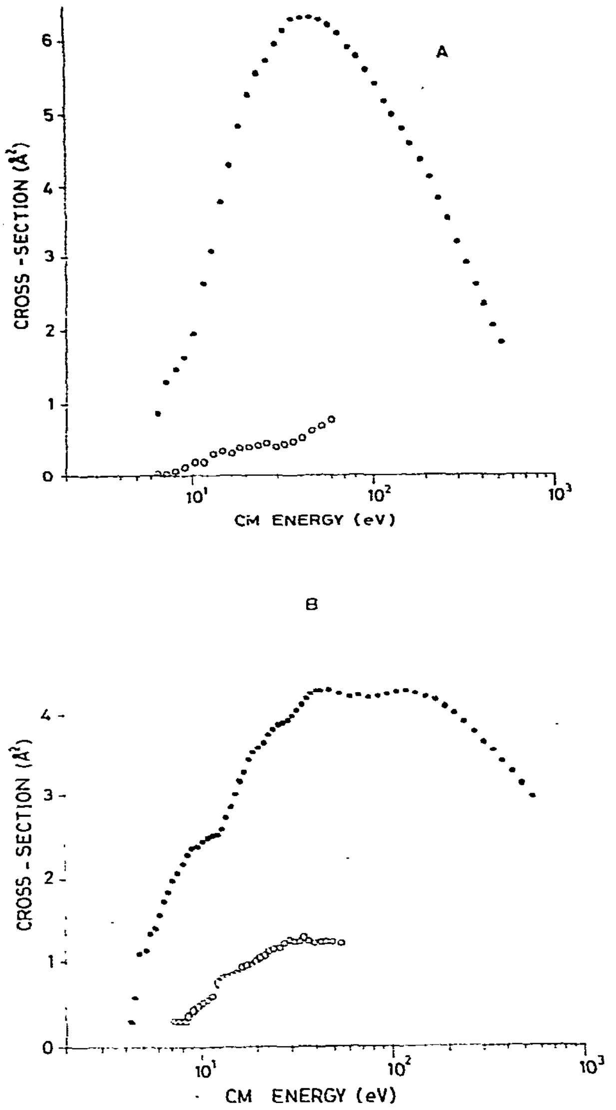

Fig. 4. Total absolute cross sections for ion (full circles) and electron (open circles) production in Cs–NO collisions (A) and Cs–O$_2$ collisions (B) as a function of the center-of-mass collision energy. The cross sections are plotted in absolute units (Å^2).

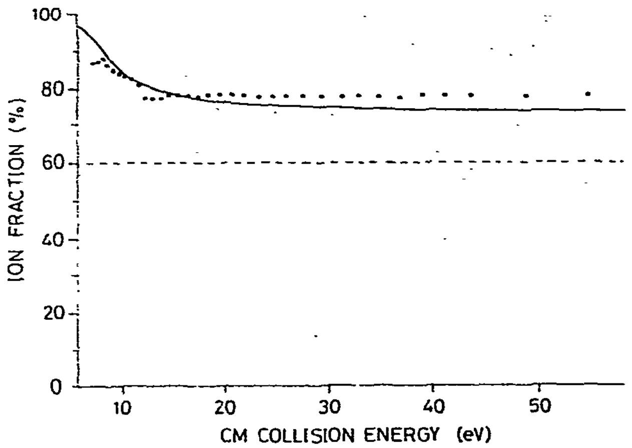

Fig. 5. The fraction of ionizing collisions between cesium atoms and O$_2$ molecules which lead to the production of stable O$_2^-$ ions as a function of the c.m. collision energy. The experimental fraction is indicated by dots. The solid line is the fraction calculated according to the modified Franck–Condon model. The dashed line is the fraction expected by the pure Franck–Condon model.

some structure while no such feature can be observed in the corresponding cross section for Cs–NO collisions. The absolute magnitude of the cross section is larger for the Cs–NO case than for Cs–O$_2$ collisions. Another difference appears in the fraction of ionizing collisions which leads to electron production for both systems. This fraction could be measured very accurately because only the ion current $G_i(E)$ and the total current $G_{i+e}(E)$ have to be known in order to obtain the value of this fraction. The measurement is independent of the target-gas pressure and, more im-

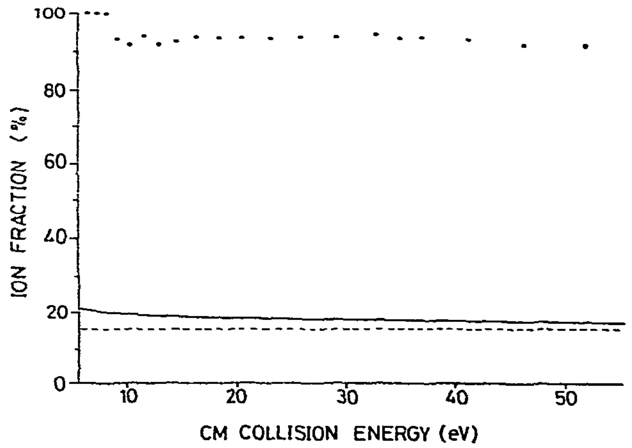

Fig. 6. The fraction of ionizing Cs–NO collisions which produce stable NO$^-$ ions. The experimental fraction is indicated by dots. The solid and dashed lines represent the fractions calculated by means of the modified and pure Franck–Condon models respectively.

portant, of the detection efficiency. In figs. 5 and 6 the fraction of ionizing collisions which leads to production of ions has been plotted as a function of the (laboratory) collision energy. From fig. 5 we observe that $\approx 77\%$ of the ionizing collisions between cesium atoms and O_2 molecules lead to ion production, while the corresponding value for Cs–NO collisions is $\approx 93\%$ (fig. 6). For collision energies higher than 60 eV these fractions are relatively weak functions of the collision energy. Nevertheless it can be observed that they do not remain completely constant at these energies.

4. Discussion

Collisions between alkali atoms and electronegative molecules like NO or O_2 are known to be attractive. The positive electron affinity of these molecules causes the curve crossing between the potentials of the covalent and ionic ground states of the atom–molecule system to occur at large atom–molecule distances. The consequence of such a large crossing radius is that the absolute magnitude of the total cross section for ion-pair formation is so large that the contribution of small-impact-parameter collisions is negligible. Another consequence of this large crossing radius is that vibrational excitation of molecular ions which are produced in such collisions is due to a curve-crossing process rather than to direct momentum transfer. This is because the force between the two molecular nuclei is not affected by the nearby atom at atom–molecule distance which are outside the repulsive part of the interaction potential.

4.1. The influence of vibration on the cross section for ion-pair formation

The structure which can be observed in the cross section for ion-pair formation in Cs–O_2 collisions (fig. 4B) has been successfully explained by Kleyn et al. [2]. We briefly recall the model which they used in order to explain this structure. The simple assumptions they made for the potential-energy surfaces belonging to the ionic and covalent ground states of the Cs–O_2 system are justified for large atom–molecule distances. The assumptions are as follows:

(1) In the covalent ground state there is no interaction between the atom and the molecule at all. The interaction between the two molecular nuclei is equal to that for the isolated molecule.

(2) The ionic ground state can be considered to consist of an atomic ion and a molecular anion. The interaction between these ions is entirely coulombic, while the force between the molecular nuclei is equal to that occurring in an isolated molecular anion [7].

These assumptions yield very simple expressions for the potentials of the covalent (V_c) and the ionic (V_i) ground states:

$$V_c(\rho) = V_{XY}(\rho), \tag{1}$$

$$V_i(R, \rho) = V_{XY^-}(\rho) - 1/R + \mathrm{IP}. \tag{2}$$

$V_{XY}(\rho)$ and $V_{XY^-}(\rho)$ denote respectively the potential energy of the isolated neutral molecule and of the isolated molecular anion as a function of the bond length ρ. The potentials $V_{XY}(\rho)$ and $V_{XY^-}(\rho)$ are defined with respect to the same zero point of energy. IP stands for the ionization potential of the alkali atom and R denotes the distance beteen the atomic nucleus and the molecular center of mass. From eqs. (1) and (2) we can easily derive an expression for the crossing radius R_c:

$$R_c = \frac{1}{\mathrm{IP} - [V_{XY}(\rho) - V_{XY^-}(\rho)]}. \tag{3}$$

We see that the crossing radius depends on the bond lengths of the molecule. During a collision the system has to pass the crossing radius twice. Before the first crossing is reached the molecule may be considered to be in its equilibrium position. At the first crossing the molecule may become ionic and because the equilibrium distance of a neutral molecule (in general) is smaller than that of the corresponding anion, the molecular nuclei start to vibrate. Because the bond length in many cases will be a periodical function of time, the crossing radius will also vary periodically in time. The diabatic transition probability is strongly dependent on the magnitude of the crossing radius because the coupling matrix element decreases exponentially with increasing crossing radius [8,9]. It will be clear that the reneutralisation probability at the second crossing is a function of the time the system spends between the two crossings during the collision. When the second crossing radius is at a maximum we expect a minimal reneutralization probability. On the other hand, if the second crossing radius is at a minimum the reneutralization probability is maximal. This feature causes the structure in the total cross section for ion-pair formation. For a detailed description we refer the reader to ref. [6]. Our measurements confirm the results of Kleyn et al.

The basic conclusions which can be drawn from Kleyn's analysis are:

(1) The motion of the molecular nuclei is well described by classical mechanics.

(2) The transition at a curve crossing is given by the "generalized" Landau–Zener model. The time needed for the transition from the covalent to the ionic surface, or vice versa, is assumed to be infinitely short in this model.

The observation that the molecular nuclei may be treated classically in order to explain the minima and maxima in the total cross section for ion-pair formation raises the question if the forementioned model is suitable to calculate the vibrational energy of the molecule after the collision. Apart from the fact that the vibrational energy of the molecule must be quantized, what may raise some problems in applying the classical model, we have to analyze if a measurement of the time-dependent behaviour of the molecular bond length a priori yields some information about the vibrational energy of the molecule. Classically, a vibrational period of a particle moving in a harmonic potential is independent of its energy. Quantum mechanically, any superposition of time-dependent vibrational eigenstates of a harmonic potential exhibits a classical behaviour of the expectation values of position and momentum, regardless the vibrational energy of the system. In order to get information about the vibrational-energy distribution one must determine the time evolution of the probability density at all internuclear distances. A measurement of the structure in the total cross section, which in principle is a measurement of the expectation value of the molecular bond length as a function of time, is too crude for this purpose.

4.2. Measurements of vibrational excitation of the molecular anion

More information about the vibrational energy of the produced ions can be obtained by measuring the total cross section for ion production as well as the total cross section for electron production. It is well known [10] that vibrationally excited molecular anions eject an electron if their total energy exceeds the zero-point energy of the neutral molecule. For NO^- molecules this is the case if the vibrational quantum number is larger than zero, while an O_2^- ion ejects an electron if its vibrational quantum number is larger than three [10]. The following reaction schemes can be set up:

$$Cs + O_2 \rightarrow Cs^+ + O_2^-(v \leqslant 3)$$
$$\rightarrow \text{ion production},$$
$$Cs + O_2 \rightarrow Cs^+ + O_2^-(v > 3)$$
$$\rightarrow Cs^+ + O_2 + e^- \rightarrow \textit{electron production},$$
$$Cs + NO \rightarrow Cs^+ + NO^-(v = 0)$$
$$\rightarrow \text{ion production},$$
$$Cs + NO \rightarrow Cs^+NO^-(v > 0)$$
$$\rightarrow Cs^+ + NO + e^- \rightarrow \text{electron production}.$$

In Cs–O_2 and Cs–NO collisions, electron production which is due to autoionization during the collision is negligible. For Cs–O_2 collisions, autoionization is possible when the total energy (electronic plus vibrational) of the ionic system $Cs^+ + O_2^-(v \geqslant 4)$ exceeds the energy of the system $Cs^+ + O_2(v = 0) + e^-$. This may occur in two cases:

(1) At large atom–molecule distances.

When assuming a coulombic force between the Cs^+ and the O_2^- ion, while no interaction is assumed between the Cs^+ atom and the O_2 molecule, the vibrational quantum number of the O_2^- molecule should be larger than 25 for autoionization of the O_2^- molecule to take place at an atom–molecule distance of 5Å. It is unlikely that the O_2^- molecule can be vibrationally excited so high.

(2) At small atom–molecule distances.

At small atom–molecule distances, there could be a crossing between the potentials of the systems $Cs^+ + O_2^-$ $(v \geqslant 4)$ and $Cs^+ + O_2$ $(v = 0)$, although such a crossing seems improbable, due to the considerable polarizability of the O_2^- ion compared to O_2^-. In case of such a crossing to occur anyhow, autoionization at small atom–molecule distances seems improbable because of the lifetime of the O_2^- ion which is comparable to a vibrational period of the molecule. The system spends a much shorter time in the repulsive region than this lifetime of vibrationally excited O_2^-.

A similar reasoning can be applied for the case of Cs–NO collisions.

It will be clear that a measurement of the branching ratio between electron and ion formation directly is a measure for the vibrational energy of the produced ions. The fraction of Cs–NO or Cs–O_2 collisions which leads to formation of stable anions has been plotted in figs. 5 and 6. The total cross section for O^- production, has been shown to be small in comparison to the total cross section for O_2^- production [2].

4.3. *The experimental results in connection with some models*

Models which describe vibrational excitation of the molecular anion in collisions between an alkali atom and O_2 or NO should explain the following features which can be observed by experiment:

The expectation value of the molecular internuclear distance has to be a function of time which is more or less corresponding with the classical motion of a particle over the potential of the molecular anion. This implies that the vibrational wave packet representing the motion of the molecular nuclei has to oscillate back and forth with the classical vibration frequency of the molecular anion, and moreover, this wave packet must be confined to a small region of internuclear distances during all time. The wave packet may not exhibit considerable dispersion during the collision.

The fraction of electrons produced in collisions between an alkali atom and O_2 or NO has to be in agreement with the experimental data. A special feature which has to be explained is that this fraction is a function of the collision energy.

Three models have been proposed previously in order to describe vibrational excitation of the molecular ion in ion-pair formation processes which we will discuss in this paper. These models are:

(i) the Franck–Condon model [*],
(ii) the modified Franck–Condon model,
(iii) the Bauer–Fisher–Gilmore model.

We confine ourselves to models which describe the population distribution over quantized vibrational states of the molecular ion. This excludes models which describe the vibrational classically from our discussion. An example of such a model is the surface hopping trajectory method.

(i) The Franck–Condon model

The simplest model which leads to a final distribution over quantized vibrational states of the molecular anion in atom–molecule collisions is the Franck–Condon model. The model assumes that the transition from the covalent to the ionic state, or the reverse, occurs so fast that the molecular nuclei cannot move during this transition. A transition which fulfills this condition is called vertical. When the system reaches the first crossing the vibrational wavefunction of the neutral molecule is given by $u_0(\rho)$, which is the zeroth-order vibrational wavefunction of the neutral molecule. Just at the time at which the molecule becomes ionic, the vibrational wavefunction of the molecular anion must have an identical shape as $u_0(\rho)$ because the molecular nuclei are not supposed to change their position during a vertical transition. If the electronic transition probability is given by P, then the normalization condition leads to the following expression for the vibrational wavefunction of the molecular ion at the time at which the transition occurs [11]:

$$\psi_{\rm vib}^{\rm ion}(\rho, t=0) = P^{1/2} u_0(\rho). \qquad (4)$$

---

[*] There might rise some confusion about the term "Franck–Condon model". We refer to the Franck–Condon model when all electronic transitions which may occur in a collision are vertical, i.e. the molecular vibration is frozen during the electronic transition. This does not exclude molecular vibration during the collision time which can be much longer than the transition time. In such a case we still speak about the Franck–Condon model if just the electronic transitions are vertical, even when the collision time is as long as a few vibrational periods of the molecule. In such a situation Gislason et al. [11] adopted the nomenclature of the "diabatic moving wave packet" model. The modified Franck–Condon model which is discussed in this paper is called the "adiabatic moving wave packet" model by Gislason et al.

The time evolution of this wavefunction can be calculated by expanding the vibrational wavefunction at $t = 0$ in an infinite set of vibrational eigenfunctions of the molecular anion, v_l, each having their proper time-dependent phase [11]:

$$\psi^{\rm ion}_{\rm vib}(\rho, t) = P^{1/2}\sum_l |\, v_l\rangle\langle v_l|u_0\rangle \times \exp\left[-i\omega\left(l+\tfrac{1}{2}\right)t\right]. \tag{5}$$

The probability to populate the lth vibrational state of the molecular anion is given by:

$$P_l = P|\langle v_l|u_0\rangle|^2. \tag{6}$$

The fraction of ions which are produced in a vibrational level which is stable against electron detachment can be calculated according to the formula:

$$F_{\rm i} = P\sum_{l=0}^{m}\langle v_l|u_0\rangle^2 / P\sum_{l=0}^{\infty}\langle v_l|u_0\rangle^2 = \sum_{l=0}^{m}\langle v_l|u_0\rangle^2. \tag{7}$$

m is the vibrational quantum number of the highest vibrational state which is stable against electron detachment.

The transition probability P is given by the Landau–Zener formula. The crossing radius R_c at which the transition occurs is assumed to be identical with R_c calculated from formula (3) in which one replaces ρ by the expectation value of the position calculated from formula (5). For the first crossing ρ is taken as the equilibrium distance of the neutral molecule ρ_e.

The time-dependent vibrational wavefunction in (5) has the property that the expectation value of the internuclear distance is a periodical function of time, and the length of a vibrational period is just a classical period. Moreover it can be deduced that the vibrational wave packet remains confined to a small region of internuclear distances in the case of a harmonic potential. The crossing radius at the second crossing can be calculated by taking the expectation value of the internuclear distance at the time the system passes the second crossing. The reneutralisation probability at the second crossing can be calculated in a complete analogous way as has been done for the first crossing.

This model fulfils the condition that the expectation value of the internuclear distance evolves in a classical way, and therefore it is able to explain the structure in the ionproduction cross section for Cs–O_2 collisions. On the other hand, if we analyse our measured branching ratios between electron and ion production we must conclude that there is poor agreement between the model and experiment. According to formula (7) we expect an ion fraction of ≈ 60% for Cs–O_2 collisions, while we measure a value of ≈ 77%. For collisions between cesium atoms and NO molecules the situation is even worse. An ion fraction of 16% is expected from the Franck–Condon model while the experimental value ranges between 100 and 90%. Moreover, according to the Franck–Concon model this branching ratio cannot depend on the collision energy (formula (7)). We observe an ion fraction which depends on the collision energy. This behaviour is even more pronounced in collisions between K or Na atoms and NO or O_2 molecules [13].

(ii) The modified Franck–Condon model

The Franck–Condon model has been revised by Gislason et al. [11] in order to explain the feature that low energetic collisions between an atom and a molecule lead to production of molecules which are less vibrationally excited than expected by the Franck–Condon model. The basic idea of the revision of the Franck–Condon model is that in reality the electronic transition takes a finite time during which the molecular nuclei can move. The transition time was defined by Gislason et al. to be the time during which the system passes through the static width of the coupling region, and therefore it is inversely proportional to the collision velocity. During the transition time the molecular nuclei are supposed to move classically along the adiabatic potential-energy surface. This will result in an increase of the bond length of the molecule. The second assumption which was made is that the center of the vibrational wavefunction of the neutral molecule follows the classical motion of the molecular nuclei along the adiabatic surface without any dispersion of the vibrational wave packet itself. For this reason we know both the shape and the position of the vibrational wave packet at the time at which the molecule becomes ionic. Thus:

$$\psi_{\mathrm{vib}}^{\mathrm{ion}}(\rho, t=0)=u_0(\rho-\rho_d), \qquad (8)$$

in which u_0 denotes the vibrational wavefunction of the neutral molecule which is shifted by an amount ρ_d towards larger internuclear distance. This wavefunction may be expanded into vibrational eigenstates of the molecular anion, just as has been done in formula (5). The fact that the Franck–Condon overlap factors are strongly dependent on ρ_d causes the probability of finding the molecular ion in a certain vibrational state to be shifted towards lower-lying states in comparison to the Franck–Condon model. At high velocities the modified Frank–Condon model tends to the pure Franck–Condon model because ρ_d becomes small due to the short transition time during which the molecule may stretch its bond.

The effect of an increase in effective bond length of the molecule at a curve crossing has been observed experimentally by Aten and Los [13] in low energetic alkali–halogen collisions. At higher energies this effect, which is called prestretching, became negligible.

The modified Franck–Condon model explains, just like the pure Franck–Condon model, the structure in the ion production cross section in Cs–O_2 collisions. This model also predicts a branching ratio between electron and ion production which is a function of the collision velocity. Using this model we did a calculation for the passage through only one curve crossing in collisions between cesium atoms and O_2 and NO molecules. As ions or electrons are produced by a single-electron transfer, bond stretching does not affect the vibrational state of the molecular anion according to the modified Franck–Condon model. Therefore according to this model the branching radio between electron and ion production is the result of a single passage through a crossing region. The fact that only crossing is taken into account, while in real collisions two crossings have to be passed, neglects the detailed influence of orientational effects in these collisions. The coupling matrix element which determines the width of the static-coupling region and thereby the transition time depends on the orientation of the molecular axis relative to the radius vector connecting the molecular center of mass with the atomic nucleus [14]. We took a mean value of half the coupling matrix element in order to correct for the orientation effect. Moreover the radial velocity at the curve crossing depends on the impact parameter. We chose an effective impact parameter which is equal to $R_c/2^{1/2}$.

Although we are aware of the fact that this calculation only gives an approximate value for the branching ratio, we think that it is accurate enough to decide if the model can predict the right value for real collisions. In figs. 5 and 6 we have plotted the branching ratio between electron and ion production as a function of the collision energy. The modified Franck–Condon model gives a good explanation for the branching ratio in Cs–O_2 collisions *. For Cs–NO collisions there is some improvement with respect to the Franck–Condon model, but still there is severe disagreement with the experimental results. Unless we assume unphysically large coupling matrix elements (> 1 eV), which is doubtful because the maximum of the cross section for ion-pair formation lies at a rather low collision energy, the modified Franck–Condon model cannot predict more than 30% of ions to be formed in Cs–NO collisions. Our conclusion concerning the modified Franck–Condon model is that this model is in good agreement with the experimental results for Cs–O_2 collisions but that it cannot explain the anomalous branching ratio between electron and ion formation in Cs–NO collisions. The general conclusion for this model can be that it may be a valuable improvement of the pure Franck–Condon model in certain cases.

(iii) The Bauer–Fisher–Gilmore model

We discuss the Bauer–Fisher–Gilmore model [15] in order to see if this model can predict a branching ratio between electron and ion production, which is velocity dependent, together with the motion of the molecular nuclei during the collision. That the BFG model predicts a branching ratio which is velocity dependent is obvious. At

---

* The value of the coupling matrix element in our Cs–O_2 calculations is taken from the work of Kleyn et al. [2].

the lowest collision velocities only ions should be produced while considerable vibrational excitation can be expected if the collision velocity is very high. The Bauer–Fisher–Gilmore model, however, cannot explain an oscillatory behaviour of the total cross section for ion-pair formation in Cs–O_2 collisions as a function of collision energy. For this reason we abandon the BFG model for explaining our measurements.

4.4. The absolute magnitude of the total cross section

The total cross section for ion production in Cs–O_2 collisions reaches a maximum value of 4.2 Å^2 at a center-of-mass collision energy of 130 eV. This absolute value can be compared with some theoretical approaches. The first model from which we obtain an estimate for the absolute magnitude of the total cross section for ion production is the rigid-molecule model. In this case the effect of bond stretching is completely ignored. The coupling matrix element is taken to be of the form $H_{12}^0 \sin 2\theta$, where θ denotes the angle between the molecular center of mass with the atomic nucleus. The electronic transition is assumed to be vertical and to occur at the diabatic crossing point between the potentials of the covalent and ionic ground states. The transition probability is given by the Landau–Zener formula. Using this model we expect a maximum value of the cross section for ion-pair formation of 6.9 Å^2. Taking an electron fraction of $\approx 25\%$ we expect that the total cross section for ion production will be 5.2 Å^2, which is larger than observed experimentally. The classical model used by Kleyn et al. [2] predicts a maximum value of ≈ 9.2 Å^2 (when the electron fraction is taken to be 25%) for the cross section of ion production. The larger value is due to the fact that bond stretching is taken into account in this model which decreases the averaged reneutralisation probability at the outgoing crossing which has to be passed during the collision. Applying the Magnus approximation Hickman [16] calculates a maximum value of 11 Å^2.

Table 1
Listing of the most important products that may be formed in Cs–O_2 and Cs–NO collisions (column 1), the number, symmetries and multiplicities of the electronic states of the temporarily formed triatomic molecule leading to these products (column 2), and the threshold energies (eV) for their production

$Cs(^2S)+O_2(^3\Sigma^-)$	$^4A''+^2A''$	0
$Cs(^2S)+O_2^*(^1\Delta)$	$^2A'+^2A''$	0.982
$Cs^*(^2P)+O_2(^3\Sigma^-)$	$2\times{}^4A''+2\times{}^2A''+^2A'+^4A'$	1.34
$Cs^+(^1S)+O_2^-(^2\Pi)$	$^2A'+^2A''$	3.45
$Cs(^2S)+NO(^2\Pi)$	$^3A'+^3A''+^1A'+^1A''$	0
$Cs^*(^2P)+NO(^2\Pi)$	$3\times{}^3A''+3\times{}^3A'+3\times{}^1A''+3\times{}^1A'$	1.34
$Cs^+(^1S)+NO^-(^3\Sigma^-)$	$^3A''$	3.89
$Cs^+(^1S)+NO^{*-}(^1\Delta)$	$^1A''+^1A'$	4.64
$Cs^+(^1S)+NO^{*-}(^1\Sigma^+)$	$^1A'$	5.05

The relatively small absolute magnitude of the cross section might be due to coupling with excited states. Kempter et al. [17] have shown that the cross sections for alkali excitation in collisions between K or Na atoms and O_2 or NO molecules are appreciable with respect to the estimated magnitudes of the ion-pair formation cross sections. In table 1 we give a list of the possible exit channels in collisions between cesium atoms and NO or O_2 molecules. It can be seen that for the Cs–O_2 case coupling may occur to an electronic state which results in production of excited oxygen molecules. Because this state crosses with the ionic ground state at a relatively small atom–molecule distance, coupling between these states will be appreciable. In our calculations it has been taken into account that only 1/3 of the incoming Cs–O_2 collisions are having the proper electronic symmetry for coupling with the ionic ground state to be possible.

The cross section for ion-pair formation in Cs–NO collisions reaches a maximum value of 6.9 Å^2 at a collision energy (c.m.) of 45 eV. Because predominantly NO^- ($v=0$) is produced, and moreover, there is not any structure observed in the total cross section for ion production, it seems reasonable to assume that bond stretching is unimportant in Cs–NO collisions. Using the rigid–molecule model, and neglecting coupling with electronically excited states we obtained a maximum value for the ion-pair formation cross section of 6.4 Å^2. From table 1 we can see that only 3/8 of the entrance channels have the proper symmetry to couple with the ionic ground state. The calculated maximum value is somewhat smaller than the observed one. In addition the maximum value of the cross section is calculated by assuming that the electronic transition occurs at an atom–molecule distance for which the vibronic energies of the states $|\text{cov}, v = 0\rangle$ and $|\text{ion}, v = 0\rangle$ are resonant (the BFG model). We find a value of 7.7 Å^2 which is larger than observed experimentally. Like in the Cs–O_2 case coupling can occur between the ionic ground state and the states leading to production of excited cesium atoms. Coupling to excited states which lead to production of excited neutral NO molecules is, however, improbable as can be seen from table 1. This might be the explanation for the smaller discrepancy between the experimental and theoretical value of the total cross section of ion production in Cs–NO collisions.

5. Conclusion

As a conclusion we may state that there exists not any model to date which can describe the total cross sections for electron and ion production in Cs–NO or Cs–O_2 collisions completely. Especially the experimental observation that Cs–NO collisions lead predominantly to the production of $NO^-(v = 0)$ ions gives rise to theoretical problems. The role of coupling to electronically excited states in Cs–NO and Cs–O_2 collisions has to be investigated in order to explain the observed magnitudes of the total cross sections for ion and electron production in these collisions. In the following paper total cross sections and vibrational distributions of molecular ions will be calculated applying a close-coupling model.

Acknowledgement

The authors wish to thank Mr. C.H. van Oven and Mr. L. de Boer for their technical assistance during the experimental work. Mr. M.R. Spalburg is thanked for performing the numerical calculations. This work is part of the research program of the "Stichting voor Fundamenteel Onderzoek der Materie" (Foundation for Fundamental Research on Matter) and was made possible by the financial support from the "Nederlandse Organisatie voor Zuiver-Wetenschappelijk Onderzoek" (Netherlands Organization for the Advancement of Pure Research).

References

[1] A.W. Kleyn, V.N. Khromov and J. Los, Chem. Phys. 52 (1980) 65.
[2] A.W. Kleyn, M.M. Hubers and J. Los, Chem. Phys. 34 (1978) 55.
[3] M.M. Hubers, A.W. Kleyn and J. Los, Chem. Phys. 17 (1976) 303.
[4] A.P.M. Baede and J. Los, Physica 52 (1971) 422.
[5] J.A. Aten and J. Los, J. Phys. E8 (1975) 408.
[6] J. Los and A.W. Kleyn, in: Alkali halide vapors, eds. P. Davidovits and D.L. McFadden (Academic Press, New York, 1979) p. 275.
[7] L. Andrews, Appl. Spectry. Rev. 11 (1976) 125.
[8] R.E. Olson, F.T. Smith and E. Bauer, Appl. Opt. 10 (1971) 1848.
[9] R. Grice and D.R. Herschbach, Mol. Phys. 27 (1974) 159.
[10] G.J. Schultz, Rev. Mod. Phys. 45 (1973) 423.
[11] E.A. Gislason, A.W. Kleyn and J. Los, Chem. Phys. 59 (1981) 91.
[12] U.C. Klomp and J. Los, Chem. Phys. 71 (1982) 443.
[13] J.A. Alten and J. Los, Chem. Phys. 25 (1977) 47.
[14] E.A. Gislason and J.G. Sachs, J. Chem. Phys. 62 (1975) 2678.
[15] E. Bauer, E. Fisher and F. Gilmore, J. Chem. Phys. 51 (1969) 4173.
[16] A.P. Hickman, J. Chem. Phys. 72 (1980) 4413.
[17] V. Kempter, W. Mecklenbrauck, M. Menzinger and C.H. Schlier, Chem. Phys. Letters 11 (1971) 353.